LECTURE 14: THE MEASUREMENT OF RSD

GONG-BO ZHAO

Learning goals

After this lecture, students should be able to:

- explain the physical origin of redshift-space distortions and derive the linear Kaiser multipoles;
- interpret the TNS model as an intermediate-level template between linear theory and modern EFT analyses;
- distinguish standard template fitting, ShapeFit compression, and EFT full modelling;
- write down the schematic ingredients of a DESI-like full-shape likelihood, including the survey window, nuisance parameters, and post-reconstruction BAO information;
- describe why recent DESI analyses are moving beyond the power spectrum alone, for example by including the bispectrum or the cross-information between pre- and post-reconstruction fields.

1. From linear RSD to realistic analyses

In real space, a galaxy sits at comoving position $\mathbf{x}$, but in redshift space its radial peculiar velocity shifts the inferred line-of-sight position. In the plane-parallel limit,

$$\mathbf{s} = \mathbf{x} + \frac{v_\parallel(\mathbf{x})}{aH}\hat{\mathbf{n}}, \tag{1}$$

where $\hat{\mathbf{n}}$ is the line-of-sight direction. Mass conservation then implies that anisotropy appears in Fourier space even if the real-space clustering is statistically isotropic.

At linear order, one obtains the Kaiser formula [15],

$$P_g^{s,\mathrm{lin}}(k,\mu) = \left(b_1 + f\mu^2\right)^2 P_{\mathrm{L}}(k), \tag{2}$$

where b_1 is the linear galaxy bias, $f \equiv d\ln D/d\ln a$ is the linear growth rate, $\mu \equiv \hat{\mathbf{k}}\cdot\hat{\mathbf{n}}$, and $P_{\mathrm{L}}(k)$ is the linear matter power spectrum. The observable anisotropy is usually discussed in terms of Legendre multipoles,

$$P_\ell(k) = \frac{2\ell+1}{2}\int_{-1}^{1} d\mu\, P(k,\mu)\mathcal{L}_\ell(\mu). \tag{3}$$

For the Kaiser model the lowest three non-zero multipoles are

$$P_0(k) = \left(b_1^2 + \frac{2}{3}b_1 f + \frac{1}{5}f^2\right) P_{\rm L}(k), \tag{4}$$

$$P_2(k) = \left(\frac{4}{3}b_1 f + \frac{4}{7}f^2\right) P_{\rm L}(k), \tag{5}$$

$$P_4(k) = \frac{8}{35}f^2 P_{\rm L}(k). \tag{6}$$

This already shows two important facts. First, RSD is intrinsically anisotropic and therefore needs at least a monopole and quadrupole, and often also a hexadecapole, to be measured. Second, the quantity most tightly constrained by a two-point analysis is usually a growth-amplitude combination such as $f\sigma_8$, rather than f and σ_8 separately.

However, the linear expression is not accurate enough for modern surveys. On quasi-linear scales the observed anisotropy is affected by nonlinear density evolution, nonlinear bias, velocity dispersion along the line of sight, Alcock-Paczynski (AP) distortions, the survey window function, and observational systematics such as fiber assignment. This is why practical RSD work is really a *full-shape* problem: one must forward-model the entire anisotropic clustering signal, not just a single feature.

2. The TNS model

The RSD is much more difficult to measure accurately, simply because it is harder to model the velocity power spectrum properly, even on linear scales. The commonly used model, or template, of the RSD is called the TNS model [4].

$$\begin{aligned} P_{\rm g}(k,\mu,z) =& D_{\rm FOG}\left(k,\mu_2,z\right)\left[P_{{\rm g},\delta\delta}(k,z)\right. \\ &+ 2f(z)\mu^P P_{{\rm g},\delta\theta}(k,z) + f^2(z)\mu^4 P_{\theta\theta}(k,z) \\ &\left.+ A(k,\mu,z) + B(k,\mu,z)\right] \end{aligned} \tag{7}$$

where,

$$\begin{aligned} P_{{\rm g},\delta\delta}(k,z) =& b_1^2(z)P_{\delta\delta}(k,z) + 2b_1(z)b_2(z)P_{{\rm b2},\delta}(k,z) \\ &- \frac{8}{7}b_1(z)\left(b_1(z)-1\right)P_{{\rm bs2},\delta}(k,z) \\ &+ \frac{64}{315}b_1(z)\left(b_1(z)-1\right)\sigma_3^2(k,z)P_m^{\rm L}(k,z) \\ &+ b_2^2(z)P_{\rm b22}(k,z) - \frac{8}{7}\left[b_1(z)-1\right]b_2(z)P_{\rm b2s2}(k,z) \\ &+ \frac{16}{49}\left[b_1(z)-1\right]^2 P_{\rm bs2}(k,z) \end{aligned} \tag{8}$$

$$
\begin{aligned}
P_{\mathrm{g},\delta\theta}(k,z) =& b_1(z)P_{\delta\theta}(k,z) + b_2(z)P_{\mathrm{b2},\theta}(k,z) \\
&- \frac{4}{7}\left[b_1(z)-1\right]P_{\mathrm{bs2},\theta}(k,z) \\
&+ \frac{32}{315}\left[b_1(z)-1\right]\sigma_3^2(k,z)P_m^{\mathrm{L}}(k,z)
\end{aligned}
\tag{9}
$$

$$
\begin{aligned}
P_{\mathrm{g},\theta\theta}(k,z) &= P_{\theta\theta}(k,z) \\
D_{\mathrm{FoG}}(k,\mu,z) &= \left\{1 + \left[k\mu\sigma_v(z)\right]^2/2\right\}^{-2} \\
A(k,\mu,z) &= b_1^3(z)\sum_{m,n=1}^{3}\mu^{2m}\left[f(z)/b_1(z)\right]^n A_{mn}(k,z) \\
B(k,\mu,z) &= b_1^4(z)\sum_{m=1}^{4}\sum_{a,b=1}^{2}\mu^{2m}\left[-f(z)/b_1(z)\right]^{a+b} B_{ab}^m(k,z)
\end{aligned}
\tag{10}
$$

$$
\begin{aligned}
b_{\mathrm{s2}} &= -\frac{4}{7}\left(b_1-1\right) \\
b_{\mathrm{3nl}} &= \frac{32}{315}\left(b_1-1\right)
\end{aligned}
\tag{11}
$$

2.1. **How to read the TNS formula.** The TNS model can be read in layers. The first three terms,

$$
P_{\mathrm{g},\delta\delta} + 2f\mu^2 P_{\mathrm{g},\delta\theta} + f^2\mu^4 P_{\theta\theta},
\tag{12}
$$

are the nonlinear extension of the Kaiser density-density, density-velocity and velocity-velocity contributions. The extra A and B terms encode mode-coupling corrections generated by nonlinear redshift-space mapping [4]. Finally, the multiplicative damping factor D_{FoG} accounts phenomenologically for small-scale random motions along the line of sight, the so-called Fingers-of-God effect.

This is why the TNS expression has remained so influential. It is complicated enough to go beyond the linear Kaiser limit, yet simple enough to be used as a practical fitting template. Historically, many BOSS and eBOSS $f\sigma_8$ measurements used this style of modelling [5, 6, 7]. Pedagogically, it is useful to regard TNS as a bridge between the classic BAO+RSD template era and the more recent EFT full-modelling era.

2.2. **From a theory model to an observable data vector.** A power-spectrum model by itself is not yet the quantity fitted to survey data. As discussed in the previous lecture, the survey geometry and estimator act on the theory through a forward model. In a compact notation one may write

$$
\mathbf{d}_{\mathrm{th}} = \mathbf{W}\,\mathbf{t}(\alpha_\perp, \alpha_\parallel, \boldsymbol{\vartheta}_{\mathrm{cosmo}}, \boldsymbol{\vartheta}_{\mathrm{nuis}}),
\tag{13}
$$

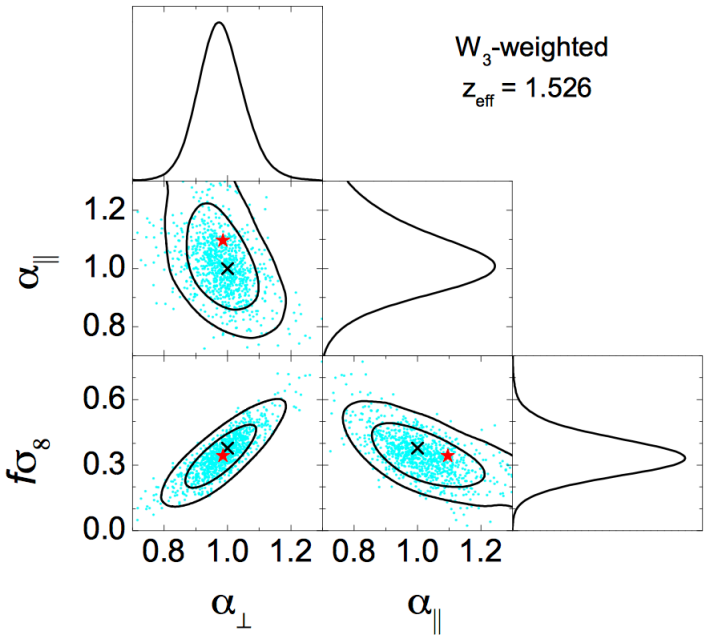

FIGURE 1. The BAO and RSD fit in k-space using BOSS DR14 quasar mock data [5].

where $\mathbf{t}$ is the unconvolved theoretical multipole vector, $\mathbf{W}$ is the survey-window operator, $\alpha_{\perp,\parallel}$ describe AP distortions, and $\boldsymbol{\vartheta}_{\rm nuis}$ contains bias, FoG and broadband nuisance parameters. The Gaussian likelihood is then

$$\chi^2 = (\mathbf{d} - \mathbf{d}_{\rm th})^T \mathbf{C}^{-1} (\mathbf{d} - \mathbf{d}_{\rm th}). \tag{14}$$

This equation is deliberately simple, but it is the conceptual backbone of almost every modern full-shape analysis, including DESI [18, 9].

There are two approaches for the full-shape analysis: A) a fixed-template analysis and B) a full-modeling analysis.

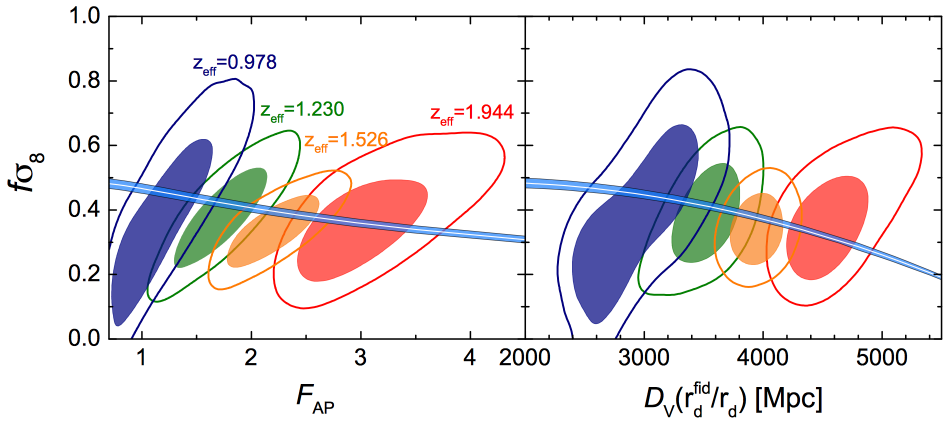

FIGURE 2. The BAO and RSD fit in k-space using the actual BOSS DR14 quasar data [5].

3. A fixed-template analysis

A fixed-template analysis means that the 'model' used for the full-shape analysis has a fixed shape, generated using a fiducial cosmology. This is why it is called a 'template' instead of 'model'. Traditional measurements for $f\sigma_8$ follow this approach, including the works in [5, 6, 7].

Recently, a new approach called 'ShapeFit' [8] was developed to extend the applicability of the fixed-template analysis, which can be regarded as an improved version of the fixed-template analysis (but it is still a fixed-template analysis). The new DESI analysis took this approach [9].

3.1. What is really varied in a fixed-template fit.

In a traditional template analysis, the broadband shape of the theoretical spectrum is inherited from one fiducial cosmology and is not recomputed from scratch at every likelihood step. Instead, the fit varies a relatively small set of physically transparent parameters, typically AP scalings, a growth-amplitude combination, bias amplitudes and broadband nuisance coefficients:

$$\mathbf{d}_{\rm th}^{\rm temp} = \mathbf{W}\,\mathbf{t}_{\rm fid}(\alpha_\perp, \alpha_\parallel, f\sigma_8, \boldsymbol{\eta}). \tag{15}$$

This makes the fit fast and robust, which is one reason template methods were so successful for BOSS and eBOSS. The price is that one does not let the cosmological model reshape the full transfer function directly. Therefore a conventional template fit is excellent for measuring geometric and growth combinations, but less direct for constraining the underlying cosmological parameters themselves.

3.2. **ShapeFit as an extended template analysis.** ShapeFit was introduced to bridge part of the gap between the traditional compressed BAO+RSD approach and a direct cosmological full-modelling fit [8, 16]. A convenient schematic way to write the ShapeFit deformation is

$$P_{\rm lin}^{\rm SF}(k) \propto P_{\rm lin}^{\rm fid}(k)\,\exp\left[\frac{m}{a}\tanh\left(a\ln\frac{k}{k_p}\right)+n\ln\frac{k}{k_p}\right], \tag{16}$$

with a pivot scale k_p chosen near the matter-radiation equality scale and with a fixed to a value such as $a \simeq 0.6$ in practical implementations. The parameter m controls the local slope around the pivot and therefore captures information related to the equality scale, while n behaves more like an overall tilt parameter. In DESI DR1, one effectively varies a single shape degree of freedom because the two are strongly anti-correlated [9].

This is a very elegant idea. ShapeFit keeps the computational and interpretational advantages of a compression approach, but it recovers much more of the broadband information than the older standard $(\alpha_\perp, \alpha_\parallel, f\sigma_8)$ compression. In this sense it is still a fixed-template method, but it is a much more informative one. For a Stage-IV survey, this middle ground is extremely attractive: fast enough to validate on many mocks, but much closer in information content to direct cosmological fitting.

3.3. **When is a fixed-template analysis especially useful?** Template approaches remain especially useful in three situations. First, they are ideal when the immediate goal is to quote robust late-time observables such as distances and growth combinations with minimal dependence on early-Universe assumptions. Second, they are computationally cheap, which makes them easy to test over many survey realizations and systematic variations. Third, they provide an intuitive compression that is often closer to what one wants to display in summary plots. Their main weakness is that once the true cosmology moves significantly away from the fiducial template, or once one wants to explore extensions that truly reshape the transfer function, direct full modelling becomes more natural.

4. A full-modeling analysis

A full-modeling analysis means that the shape of the model varies with cosmological parameters, which is more robust but computationally more expensive. In this approach, the theory model of EFTofLSS [10] is widely used. Recent implications include [9, 11, 12, 13].

4.1. **A schematic EFT decomposition.** The EFT point of view is that we should not pretend to know all small-scale physics exactly. Instead, we write the large-scale galaxy field as a bias expansion plus effective corrections that absorb unresolved short-distance effects. Schematically,

$$\delta_g(\mathbf{x}) = b_1\delta + \frac{b_2}{2}\delta^2 + b_{s^2}s^2 + b_{3\mathrm{nl}}O_3 + \epsilon + \cdots , \tag{17}$$

and in redshift space one writes the anisotropic power spectrum as

$$P_g^{s,\mathrm{EFT}}(k,\mu) = P^{s,\mathrm{IR}}_{\mathrm{tree+1loop}}(k,\mu) + P_{\mathrm{ctr}}(k,\mu) + P_{\mathrm{stoch}}(k,\mu). \tag{18}$$

Here $P^{s,\mathrm{IR}}_{\mathrm{tree+1loop}}$ denotes the perturbative prediction, including the usual infrared resummation that treats the BAO damping correctly, P_{ctr} contains counterterms, and P_{stoch} contains shot-noise-like and other stochastic corrections [10, 17, 11].

A useful schematic form is

$$\begin{aligned} P_{\mathrm{ctr}}(k,\mu) &\sim -2k^2 P_{\mathrm{lin}}(k)\left(c_0 + c_2\mu^2 + c_4\mu^4 + \cdots\right), \\ P_{\mathrm{stoch}}(k,\mu) &\sim P_{\mathrm{shot}} + s_2k^2 + s_{2\mu}k^2\mu^2 + \cdots . \end{aligned} \tag{19}$$

where the coefficients c_i and s_i are nuisance parameters marginalized over in the fit. The exact basis differs from code to code, but the logic is universal: as one pushes to higher k, the missing short-distance physics first appears as smooth corrections with increasing powers of k.

The BAO part of the signal is usually treated with infrared resummation, which may be written schematically as

$$P_{\mathrm{wig}}(k,\mu) \to \exp\left[-\frac{k^2\Sigma^2(\mu)}{2}\right] P_{\mathrm{wig}}(k,\mu), \qquad \Sigma^2(\mu) = \Sigma_\perp^2 + \mu^2\left(\Sigma_\parallel^2 - \Sigma_\perp^2\right). \tag{20}$$

This is one of the reasons EFT-style models are conceptually cleaner than older templates: the smoothing of the BAO by large bulk flows is treated in a systematic expansion rather than inserted by hand.

4.2. **A DESI-like full-shape likelihood.** A modern DESI-style analysis does not fit only the pre-reconstruction power spectrum, and it does not ignore the survey window. A simple schematic likelihood can be written as

$$\mathbf{d} = \left(P_0^{\mathrm{pre}}, P_2^{\mathrm{pre}}, P_4^{\mathrm{pre}}, \alpha_\perp^{\mathrm{post}}, \alpha_\parallel^{\mathrm{post}}\right)^T, \tag{21}$$

$$\mathbf{d}_{\mathrm{th}}(\boldsymbol{\theta}) = \left(\mathbf{W}\,\mathbf{t}_{\mathrm{pre}}(\boldsymbol{\theta}, \boldsymbol{b}, \boldsymbol{c}, \boldsymbol{s}), \alpha_\perp(\boldsymbol{\theta}), \alpha_\parallel(\boldsymbol{\theta})\right)^T, \tag{22}$$

$$\chi^2 = (\mathbf{d} - \mathbf{d}_{\mathrm{th}})^T \mathbf{C}_{\mathrm{tot}}^{-1} (\mathbf{d} - \mathbf{d}_{\mathrm{th}}), \qquad \mathbf{C}_{\mathrm{tot}} = \mathbf{C}_{\mathrm{stat}} + \mathbf{C}_{\mathrm{sys}}. \tag{23}$$

The first block describes the pre-reconstruction full-shape information, while the second block adds the sharpened post-reconstruction BAO constraints. This is a very practical strategy: pre-reconstruction data retain the broadband growth and RSD information, whereas post-reconstruction statistics measure the acoustic scale more cleanly [19, 9, 27].

For DESI DR1 the measurement paper uses more than 4.7 million galaxy and quasar redshifts in six redshift bins over roughly 7,500 square degrees, and reports a combined precision of about 4.7% on the amplitude of the RSD signal in a compressed analysis [9]. In the direct cosmological interpretation, the DESI full-shape plus BAO combination with simple early-Universe priors already gives highly competitive constraints on Ω_m, H_0 and σ_8 [9, 12].

4.3. **Why full modelling is powerful, and why it is hard.** The main advantage of full modelling is obvious: cosmological parameters are fit directly, so the entire broadband shape, the BAO scale, and the anisotropic RSD information are used in one coherent likelihood. This is particularly attractive for models beyond the minimal six-parameter ΛCDM picture, for massive neutrinos, or for modified gravity, where one really wants the theory prediction itself to change as the cosmological parameters vary [12, 13].

The cost is equally obvious. One must validate the perturbative model, the scale cuts, the nuisance priors, and the covariance model very carefully. This is why DESI invested so much effort in companion validation papers using `velocileptors`, `FOLPS`, `PyBird`, and configuration-space approaches [21, 22, 23, 24, 25]. A very important modern lesson is that modelling systematics are often best propagated at the level of the data covariance, for example by adding a systematic term such as

$$\mathbf{C}_{\rm tot} = \mathbf{C}_{\rm stat} + \mathbf{C}_{\rm HOD} + \cdots , \tag{24}$$

rather than only inflating final parameter error bars after the fact [26].

4.4. **The role of the survey window and fiber assignment.** In DESI, the formal likelihood above is only useful after the measurement process is modelled realistically. The survey mask, wide-angle effects and the small-angle cut used to mitigate fiber-assignment incompleteness all act through the window operator discussed in the previous lecture. In practice DESI removes pairs below $\theta \simeq 0.05^\circ$ in the full-shape power-spectrum estimator, which helps control fiber-assignment systematics but makes the raw window operation more extended in k. This is precisely why the rotated-window formalism discussed in Lecture 13 is not an optional technicality, but part of the cosmological forward model [18, 20, 9].

Recently, a new method for the RSD measurement is developed by cross-correlating the pre- and post-reconstructed density fields [14]. This is a very efficient way to extract high-order statistics from 2-point statistics.

A simple way to phrase this idea is to enlarge the two-point data vector. Instead of using only the auto-spectrum of the pre-reconstruction density field, one may consider

$$P_{\rm pre}(k,\mu) \equiv \langle \delta_{\rm pre}(\mathbf{k}) \delta^*_{\rm pre}(\mathbf{k}) \rangle, \tag{25}$$

$$P_{\rm post}(k,\mu) \equiv \langle \delta_{\rm post}(\mathbf{k}) \delta^*_{\rm post}(\mathbf{k}) \rangle, \tag{26}$$

$$P_{\times}(k,\mu) \equiv \langle \delta_{\rm pre}(\mathbf{k}) \delta^*_{\rm post}(\mathbf{k}) \rangle. \tag{27}$$

One may also define the cross-correlation coefficient

$$r(k,\mu) \equiv \frac{P_{\times}(k,\mu)}{\sqrt{P_{\rm pre}(k,\mu) P_{\rm post}(k,\mu)}}. \tag{28}$$

The point is not that reconstruction creates information from nothing. Rather, reconstruction moves some higher-order information into modified two-point statistics. A joint analysis of $(P_{\rm pre}, P_{\rm post}, P_\times)$ can therefore extract information that is inaccessible to a single auto-spectrum alone, while staying at the level of two-point summary statistics [14]. A closely related practical idea, already explored in BOSS, is to combine pre-reconstruction full-shape information with post-reconstruction BAO information in one likelihood [27].

5. Recent DESI full-shape analyses and outlook

The DESI DR1 programme is a very useful worked example because it already contains the whole modern chain: the clustering measurements and systematics studies [18], the post-reconstruction BAO measurements [19], the full-shape power-spectrum measurement paper [9], and the cosmological interpretation paper [12]. From the teaching point of view, one can think of these as four parts of a single story rather than four unrelated papers.

A striking feature of the DESI DR1 full-shape effort is how much validation preceded the cosmology result. The collaboration compared several perturbative pipelines, several parameterizations, several scale cuts, and several tracers. The general conclusion was not that all pipelines are identical, but that once each is used within a validated regime, they return mutually consistent cosmological information for DESI-like data volumes [21, 22, 23, 24, 25]. This is an extremely healthy lesson for students: modern cosmology is not just about writing down a beautiful likelihood, but about proving that it is numerically and physically trustworthy.

A second lesson is that systematic uncertainties are now handled at a much more mature level than in older analyses. For example, DESI studied the impact of halo-occupation uncertainty on full-shape inference and encoded it as an additional covariance contribution rather than as an ad hoc shift in final parameters [26]. This is precisely the right philosophy for a data set that is already in the Stage-IV regime.

5.1. Beyond the power spectrum alone.

Recent DESI-based analyses are also moving beyond the power spectrum by combining two-point and three-point information. A natural joint data vector is

$$\mathbf{d}_{\rm joint} = (\mathbf{P}_0, \mathbf{P}_2, \mathbf{P}_4, \mathbf{B}_0)^T , \tag{29}$$

where $\mathbf{B}_0$ denotes the bispectrum monopole in a chosen triangle basis. The bispectrum helps because it breaks degeneracies among growth, clustering amplitude, and nonlinear bias parameters that are difficult to separate with the power spectrum alone.

A first DESI DR1 joint power-spectrum-plus-bispectrum analysis of LRG and QSO samples showed improved compressed constraints relative to the power-spectrum-only case, especially for the growth-amplitude and broadband-shape information [28]. A 2026 cosmological follow-up using the same DESI DR1 joint data vector found that adding the bispectrum reduces the uncertainty on $\ln(10^{10}A_s)$ by about 20% relative to the power spectrum alone [29]. This is a very good example of where the field is going next: not replacing full-shape analysis, but enlarging the summary statistic beyond the power spectrum while keeping the same basic forward-modelling philosophy.

5.2. **ShapeFit or direct full modelling?** For students, the cleanest way to think about the current landscape is the following. Standard BAO+RSD template fitting is the fastest and most compressed method, but it deliberately throws away some broadband information. ShapeFit keeps the speed and much of the model independence of a template approach, while capturing most of the extra information in the shape of the linear spectrum. Direct EFT full modelling is the most straightforward route when one wants cosmological parameters themselves, especially for non-minimal models, but it demands the heaviest validation campaign. The DESI DR1 papers are important precisely because they show that all three styles of analysis can now be placed in one coherent framework.

Summary

The measurement of redshift-space distortions has evolved from the linear Kaiser picture to TNS-like nonlinear templates and then to modern EFT-style full-shape forward modelling. The TNS model remains a useful pedagogical bridge, because it makes the main physical ingredients visible: nonlinear density-velocity couplings and FoG damping. ShapeFit extends the old fixed-template strategy so that much more broadband information can be retained without fully abandoning compressed variables. EFT full modelling goes one step further and allows the cosmological model itself to reshape the entire prediction, at the cost of more nuisance parameters and much heavier validation. DESI DR1 is the best current example of how these ideas are implemented in a real survey pipeline.

Suggested reading

For the compressed-analysis point of view, start with the ShapeFit paper of Brieden, Gil-Marín and Verde [8] and its bridge-to-cosmology companion [16]. For EFT full modelling, Carrasco, Hertzberg and Senatore [10], Ivanov, Simonović and Zaldarriaga [17], and D'Amico, Senatore and Zhang [11] are good starting points. For modern survey-scale examples, the DESI DR1 full-shape measurement and cosmology papers [9, 12] are the natural references.

Homework

(1) Starting from the Kaiser formula $P_g^{s,\mathrm{lin}}(k,\mu) = (b_1 + f\mu^2)^2 P_{\mathrm{L}}(k)$, derive the monopole, quadrupole and hexadecapole. Then evaluate the coefficients for $b_1 = 2$ and $f = 0.75$.
(2) In your own words, explain the difference between a standard fixed-template analysis, a ShapeFit analysis, and a direct EFT full-modelling analysis. Which one varies the cosmological model itself at each likelihood step?
(3) Consider the schematic EFT counterterm $P_{\mathrm{ctr}} \sim -2c_0 k^2 P_{\mathrm{lin}}(k)$. If k doubles, by what factor does the prefactor k^2 change? Explain why this immediately suggests that every choice of k_{max} must be validated on mocks.
(4) Give one reason why DESI combines pre-reconstruction full-shape information with post-reconstruction BAO information, and one reason why adding the bispectrum can improve full-shape constraints further.

References

[1] M. J. Wilson, J. A. Peacock, A. N. Taylor and S. de la Torre, "Rapid modelling of the redshift-space power spectrum multipoles for a masked density field," Mon. Not. Roy. Astron. Soc. **464**, no. 3, 3121 (2017) doi:10.1093/mnras/stw2576 [arXiv:1511.07799 [astro-ph.CO]].

[2] G. B. Zhao *et al.* [BOSS Collaboration], "The clustering of galaxies in the completed SDSS-III Baryon Oscillation Spectroscopic Survey: tomographic BAO analysis of DR12 combined sample in Fourier space," Mon. Not. Roy. Astron. Soc. **466**, no. 1, 762 (2017) doi:10.1093/mnras/stw3199 [arXiv:1607.03153 [astro-ph.CO]].

[3] Y. Wang *et al.* [BOSS Collaboration], "The clustering of galaxies in the completed SDSS-III Baryon Oscillation Spectroscopic Survey: tomographic BAO analysis of DR12 combined sample in configuration space," Mon. Not. Roy. Astron. Soc. **469**, no. 3, 3762 (2017) doi:10.1093/mnras/stx1090 [arXiv:1607.03154 [astro-ph.CO]].

[4] A. Taruya, T. Nishimichi and S. Saito, "Baryon Acoustic Oscillations in 2D: Modeling Redshift-space Power Spectrum from Perturbation Theory," Phys. Rev. D **82**, 063522 (2010) doi:10.1103/PhysRevD.82.063522 [arXiv:1006.0699 [astro-ph.CO]].

[5] G. B. Zhao *et al.*, "The clustering of the SDSS-IV extended Baryon Oscillation Spectroscopic Survey DR14 quasar sample: a tomographic measurement of cosmic structure growth and expansion rate based on optimal redshift weights," Mon. Not. Roy. Astron. Soc. **482**, no. 3, 3497 (2019) doi:10.1093/mnras/sty2845 [arXiv:1801.03043 [astro-ph.CO]].

[6] F. Beutler *et al.* [BOSS], "The clustering of galaxies in the completed SDSS-III Baryon Oscillation Spectroscopic Survey: Anisotropic galaxy clustering in Fourier-space," Mon. Not. Roy. Astron. Soc. **466**, no.2, 2242-2260 (2017) doi:10.1093/mnras/stw3298 [arXiv:1607.03150 [astro-ph.CO]].

[7] G. B. Zhao *et al.* [eBOSS], "The completed SDSS-IV extended Baryon Oscillation Spectroscopic Survey: a multitracer analysis in Fourier space for measuring the cosmic structure growth and expansion rate," Mon. Not. Roy. Astron. Soc. **504**, no.1, 33-52 (2021) doi:10.1093/mnras/stab849 [arXiv:2007.09011 [astro-ph.CO]].

[8] S. Brieden, H. Gil-Marín and L. Verde, "ShapeFit: extracting the power spectrum shape information in galaxy surveys beyond BAO and RSD," JCAP **12**, no.12, 054 (2021) doi:10.1088/1475-7516/2021/12/054 [arXiv:2106.07641 [astro-ph.CO]].

[9] A. G. Adame *et al.* [DESI], "DESI 2024 V: Full-Shape Galaxy Clustering from Galaxies and Quasars," [arXiv:2411.12021 [astro-ph.CO]].

[10] J. J. M. Carrasco, M. P. Hertzberg and L. Senatore, "The Effective Field Theory of Cosmological Large Scale Structures," JHEP **09**, 082 (2012) doi:10.1007/JHEP09(2012)082 [arXiv:1206.2926 [astro-ph.CO]].

[11] G. D'Amico, L. Senatore and P. Zhang, "Limits on wCDM from the EFTofLSS with the PyBird code," JCAP **01**, 006 (2021) doi:10.1088/1475-7516/2021/01/006 [arXiv:2003.07956 [astro-ph.CO]].

[12] A. G. Adame *et al.* [DESI], "DESI 2024 VII: Cosmological Constraints from the Full-Shape Modeling of Clustering Measurements," [arXiv:2411.12022 [astro-ph.CO]].

[13] M. Ishak, J. Pan, R. Calderon, K. Lodha, G. Valogiannis, A. Aviles, G. Niz, L. Yi, C. Zheng and C. Garcia-Quintero, *et al.* "Modified Gravity Constraints from the Full Shape Modeling of Clustering Measurements from DESI 2024," [arXiv:2411.12026 [astro-ph.CO]].

[14] Y. Wang, G. B. Zhao, K. Koyama, W. J. Percival, R. Takahashi, C. Hikage, H. Gil-Marín, C. Hahn, R. Zhao and W. Zhang, *et al.* "Extracting high-order cosmological information in galaxy surveys with power spectra," Commun. Phys. **7**, no.1, 130 (2024) doi:10.1038/s42005-024-01624-7 [arXiv:2202.05248 [astro-ph.CO]].

[15] N. Kaiser, "Clustering in real space and in redshift space," Mon. Not. Roy. Astron. Soc. **227**, 1-21 (1987) doi:10.1093/mnras/227.1.1.

[16] S. Brieden, H. Gil-Marín and L. Verde, "Model-independent versus model-dependent interpretation of the SDSS-III BOSS power spectrum: Bridging the divide," Phys. Rev. D **104**, no.12, L121301 (2021) doi:10.1103/PhysRevD.104.L121301 [arXiv:2106.11931 [astro-ph.CO]].

[17] M. M. Ivanov, M. Simonović and M. Zaldarriaga, "Cosmological parameters from the BOSS galaxy power spectrum," JCAP **05**, 042 (2020) doi:10.1088/1475-7516/2020/05/042 [arXiv:1909.05277 [astro-ph.CO]].
[18] A. G. Adame *et al.* [DESI], "DESI 2024 II: Sample Definitions, Characteristics, and Two-point Clustering Statistics," JCAP **07**, 017 (2025) doi:10.1088/1475-7516/2025/07/017 [arXiv:2411.12020 [astro-ph.CO]].
[19] A. G. Adame *et al.* [DESI], "DESI 2024 III: Baryon Acoustic Oscillations from Galaxies and Quasars," JCAP **04**, 012 (2025) doi:10.1088/1475-7516/2025/04/012 [arXiv:2404.03000 [astro-ph.CO]].
[20] M. Pinon *et al.*, "Mitigation of DESI fiber assignment incompleteness effect on two-point clustering with small angular scale truncated estimators," JCAP **01**, 131 (2025) [arXiv:2406.04804 [astro-ph.CO]].
[21] M. Maus, Y. Lai, H. E. Noriega, S. Ramirez-Solano, A. Aviles, S. Chen *et al.*, "A comparison of effective field theory models of redshift space galaxy power spectra for DESI 2024 and future surveys," [arXiv:2404.07272 [astro-ph.CO]].
[22] M. Maus, S. Chen, M. White, J. Aguilar, S. Ahlen, A. Aviles *et al.*, "An analysis of parameter compression and full-modeling techniques with Velocileptors for DESI 2024 and beyond," [arXiv:2404.07312 [astro-ph.CO]].
[23] H. E. Noriega, A. Aviles, H. Gil-Marín, S. Ramirez-Solano, S. Fromenteau, M. Vargas-Magaña *et al.*, "Comparing compressed and full-modeling analyses with FOLPS: Implications for DESI 2024 and beyond," [arXiv:2404.07269 [astro-ph.CO]].
[24] Y. Lai, C. Howlett, M. Maus, H. Gil-Marín, H. E. Noriega, S. Ramírez-Solano *et al.*, "A comparison between ShapeFit compression and Full-Modelling method with PyBird for DESI 2024 and beyond," [arXiv:2404.07283 [astro-ph.CO]].
[25] S. Ramirez-Solano, M. Icaza-Lizaola, H. E. Noriega, M. Vargas-Magaña, S. Fromenteau, A. Aviles *et al.*, "Full Modeling and Parameter Compression Methods in configuration space for DESI 2024 and beyond," [arXiv:2404.07268 [astro-ph.CO]].
[26] N. Findlay, S. Nadathur, W. J. Percival, A. de Mattia, P. Zarrouk, H. Gil-Marín *et al.*, "Exploring HOD-dependent systematics for the DESI 2024 Full-Shape galaxy clustering analysis," [arXiv:2411.12023 [astro-ph.CO]].
[27] S.-F. Chen, Z. Vlah and M. White, "A new analysis of galaxy 2-point functions in the BOSS survey, including full-shape information and post-reconstruction BAO," JCAP **02**, 008 (2022) doi:10.1088/1475-7516/2022/02/008 [arXiv:2110.05530 [astro-ph.CO]].
[28] S. Novell-Masot, H. Gil-Marín, L. Verde, J. Aguilar, S. Ahlen, S. Bailey *et al.*, "Full-Shape analysis of the power spectrum and bispectrum of DESI DR1 LRG and QSO samples," [arXiv:2503.09714 [astro-ph.CO]].
[29] S. Novell-Masot, H. Gil-Marín, L. Verde, J. Aguilar, S. Ahlen, D. Bianchi *et al.*, "Cosmological constraints from the DESI DR1 joint power spectrum and bispectrum analysis," [arXiv:2603.19356 [astro-ph.CO]].